

Method for the Extraction of Partial Waves in Hadron Spectroscopy

Author: Sergi Longueira Rusiñol.

Facultat de Física, Universitat de Barcelona, Diagonal 645, 08028 Barcelona, Spain.

Advisor: Dr. Vincent Mathieu

Abstract: In this paper, we prepare and analyze a data set simulating a hadron collision experiment, to ultimately extract the partial waves of the model, exemplifying and verifying a method for this purpose to be used in hadronic physics.

I. INTRODUCTION

One of the main objectives of data analysis in hadron scattering experiments at particle accelerators is to determine the quantum properties of the resonances that occur during the reactions. These properties are associated with a partial wave value and can be calculated carrying out a partial wave expansion. Therefore, having a good method for determining these partial waves is essential.

In this report, we will focus on illustrating a possible method for the extraction of partial waves, used in practical applications and introduced by E. Barrelet in 1972 [1], exemplifying it with the historically first hadronic spectroscopy experiment: the pion-nucleon elastic scattering reaction [2]. Nevertheless, the same methodology could be applied to any two-particles reaction. Additionally, we will address the practical challenges associated with this approach and explore potential solutions.

To avoid difficulties associated with the detector, such as its acceptance, which may not be uniform, we will choose to develop a simulator to generate events following a given model. Due the well-known nature of the pion-nucleon reaction, we can use the standard partial waves values to verify that our method is well-behaved in a realistic environment. We will take as reference the measurements from the Data Analysis Center (DAC) of the Institute for Nuclear Studies (INS) at George Washington University (GWU), calculated using the SAID program, whose operation can be found in the following source: [3]. These same values will later allow us to verify that our results are consistent, which will validate the method.

II. FORMALISM OF THE PION-NUCLEON SCATTERING

We need to specify the framework within which we will be working, and for simplicity, we will consider all particles as scalars without spin components.

The differential cross-section will be proportional to the square modulus of the amplitude function [4] (Chapter 4):

$$\frac{d\sigma}{d\Omega} = \frac{1}{16\pi^2 s} |A(s, \theta, \phi)|^2, \quad (1)$$

where $s = E^2$, being E the center-of-mass energy, and

θ, ϕ are the polar and azimuthal angles respectively. The Eq. (1) is in natural units. We can use the relationship $(\hbar c)^2 = 0.389 \text{ mb} \cdot \text{GeV}^2$ [5] (Chapter 1) to convert to physical units.

Given that Lorentz invariants allow us to freely choose our reference frame and that, since the particles are not polarized, there will be no preferred direction, we can orient our axes for each event so that they always take place in a plane, and thus the amplitude does not depend on the azimuthal angle ϕ . Furthermore, because $d\Omega = d\phi \cdot d\cos(\theta)$, we know the dependence inside the function must be on $\cos(\theta)$, which from now on will be referenced as $z = \cos(\theta)$. This way, the amplitude in Eq. (1) becomes $A(s, z)$ and we can expand it in terms of Legendre polynomials $P_\ell(z)$:

$$A(s, z) = \sum_{\ell=0}^{\infty} (2\ell + 1) a_\ell(s) P_\ell(z). \quad (2)$$

$a_\ell(s)$ are the *partial waves* of the resonances with angular momentum ℓ , that can be calculated by definition as:

$$a_\ell(s) = \frac{1}{2} \int_{-1}^1 A(s, z) P_\ell(z) dz, \quad (3)$$

thanks to the orthogonality of the Legendre polynomials:

$$\int_{-1}^1 P_m(x) P_n(x) dx = \frac{2}{2n + 1} \delta_{nm}. \quad (4)$$

In a range of energy of a few GeV, the number of partial waves is limited, so we can truncate the sum in Eq. (2) to a finite number ℓ_{max} . For the purposes of this paper, we chose $\ell_{\text{max}} = 2$. That is, our model will only include S , P and D waves.

III. PROCEDURE AND RESULTS

A. Data Generation

As we have already mentioned, we need to generate the data or, more specifically, the events that in a practical scenario we would collect in the detector and will serve us to carry out all the analysis. We will consider an event as a triplet of values (s, z, ϕ) , which, given all the masses, completely defines the four-vectors of

the incoming and outgoing particles. These values are uniformly and randomly selected from their respective ranges: $s \in [s_{\min}, s_{\max}]$, $z \in [-1, 1]$ and $\phi \in [0, 2\pi]$.

We use an acceptance/rejection method to generate events following a probability distribution: $\frac{d\sigma}{d\Omega}$. To do so, we need to know the maximum value of the differential cross section, which we determine by evaluating it in a sufficiently large number of events and recording the largest value found. Then we multiply the result by a factor equal to 1.1 to ensure we do not underestimate the maximum. We proceed with the acceptance/rejection process until we reach the desired number of accepted events, N_{tot} . We chose $N_{\text{tot}} = 2 \cdot 10^5$ in this work.

In our model, $\frac{d\sigma}{d\Omega}$ is a two-variable function, and we must analyze the data considering its dependence on the two dimensions: (s, z) . We also know that the dependence on z will be polynomial ($\frac{d\sigma}{d\Omega}$ is a polynomial of order $2\ell_{\max}$ in z). Therefore, similar to what we did for the amplitude, we can expand $\frac{d\sigma}{d\Omega}$ into a series of Legendre polynomials, including in these all the dependence on the variable z . This way, all the energy dependence will be summarized in some energy-dependent factors $H_L(s)$ called *moments*:

$$\frac{d\sigma}{d\Omega}(s, z) = \sum_{L=0}^{\infty} (2L+1) H_L(s) P_L(z). \quad (5)$$

The inverse relation to obtain the moments is the following:

$$H_L(s) = \frac{1}{2} \int_{-1}^1 \frac{d\sigma}{d\Omega}(s, z) P_L(z) dz. \quad (6)$$

We can use the relation (with $C_{\ell 0; \ell' 0}^{L 0}$ being a Clebsch-Gordan coefficient)

$$\int_{-1}^1 P_{\ell}(z) P_{\ell'}(z) P_L(z) dz = \frac{2}{2L+1} |C_{\ell 0; \ell' 0}^{L 0}|^2 \quad (7)$$

to obtain the expression of the moments in terms of the partial waves

$$16\pi^2 s H_L(s) = \sum_{\ell, \ell'=0}^{\infty} \frac{|C_{\ell 0; \ell' 0}^{L 0}|^2}{2L+1} (2\ell+1)(2\ell'+1) a_{\ell}(s) a_{\ell'}^*(s), \quad (8)$$

or simply by equating Eq. (1) and Eq. (5). The expressions we arrive at are:

$$16\pi^2 s H_0(s) = |a_0(s)|^2 + 3|a_1(s)|^2 + 5|a_2(s)|^2, \quad (9a)$$

$$16\pi^2 s H_1(s) = a_0(s) a_1^*(s) + a_0^*(s) a_1(s) + 2[a_1(s) a_2^*(s) + a_1^*(s) a_2(s)], \quad (9b)$$

$$16\pi^2 s H_2(s) = a_0(s) a_2^*(s) + a_0^*(s) a_2(s) + \frac{6}{5}|a_1(s)|^2 + \frac{10}{7}|a_2(s)|^2, \quad (9c)$$

$$16\pi^2 s H_3(s) = \frac{9}{7}[a_1(s) a_2^*(s) + a_1^*(s) a_2(s)], \quad (9d)$$

$$16\pi^2 s H_4(s) = \frac{10}{7}|a_2(s)|^2. \quad (9e)$$

All moments H_i with $i > 2\ell_{\max}$ (in our case $2\ell_{\max} = 4$) will be zero.

There are many methods to determine the moments from our available data, such as the Maximum Likelihood Estimation (MLE), attempting to adjust a curve using the Chi-squared Test or χ^2 Test, or other statistical techniques found in the literature: [6, 7]. These are valid approaches and, in the limit of large numbers, allow for similar results to ours. However, we chose to create histograms in s and z , so that we could calculate Eq. (6) as the summation:

$$H_L(s_i) = \frac{1}{2} \sum_{k=1}^{n_z} \left(\frac{d\sigma}{d\Omega} \right)_{i,k} P_L(z_k) \Delta z, \quad (10)$$

with $\left(\frac{d\sigma}{d\Omega} \right)_{i,k}$ the number of accepted events with energy $s \in [s_i - \Delta s/2, s_i + \Delta s/2]$ and $z \in [z_k - \Delta z/2, z_k + \Delta z/2]$, being Δz and Δs the bin size in the variable z and s respectively, and n_z and n_s the number of bins in those variables. We chose $n_z = n_s = 30$. By doing this calculation, the value obtained for $H_L(s_i)$ depends on the total number of events, N_{tot} . This has no physical meaning, so we must introduce a normalization constant, \mathcal{C} , to convert the number of events into physical units. With that purpose, we have to calculate from our analytical model the quantity:

$$\int_{s_{\min}}^{s_{\max}} \int_{-1}^1 \frac{d\sigma}{d\Omega}(s, z) dz ds, \quad (11)$$

which we define as σ_{tot} . The constant \mathcal{C} must be such that:

$$\mathcal{C} \sum_{i=1}^{n_s} \sum_{k=1}^{n_z} \left(\frac{d\sigma}{d\Omega} \right)_{i,k} \Delta z \Delta s = \mathcal{C} N_{\text{tot}} \Delta z \Delta s = \sigma_{\text{tot}}, \quad (12)$$

so it must hold:

$$\mathcal{C} = \frac{\sigma_{\text{tot}}}{N_{\text{tot}} \Delta z \Delta s}. \quad (13)$$

We can calculate σ_{tot} analytically, since in this case we know $\frac{d\sigma}{d\Omega}(s, z)$. In a practical experiment, we would calculate the total cross-section per energy $\sigma(s)$ from the ratio N/\mathcal{L} , where \mathcal{L} is the *luminosity* and N the number of interactions with that specific energy per second, and that would allow us to finally obtain σ_{tot} .

The moments $H_L(s)$ with $L \leq 4$ and the sum from Eq. (5) completely define the differential cross-section $\frac{d\sigma}{d\Omega}$ since it is a polynomial of order $2\ell_{\max}$ in z .

In Fig. 1, we observe that the moments calculated using our method are perfectly consistent with those calculated from the model. This also indicates that our event generator works properly and that the normalization performed is accurate, as it returns the physical value from the data. We can also notice that, as the number of ℓ increases, the moments seem to become increasingly smaller. In perspective, the error bars become more significant, as their magnitude depends solely on the number of events within each energy bin, and not on the angular momentum. Another interesting aspect is that the

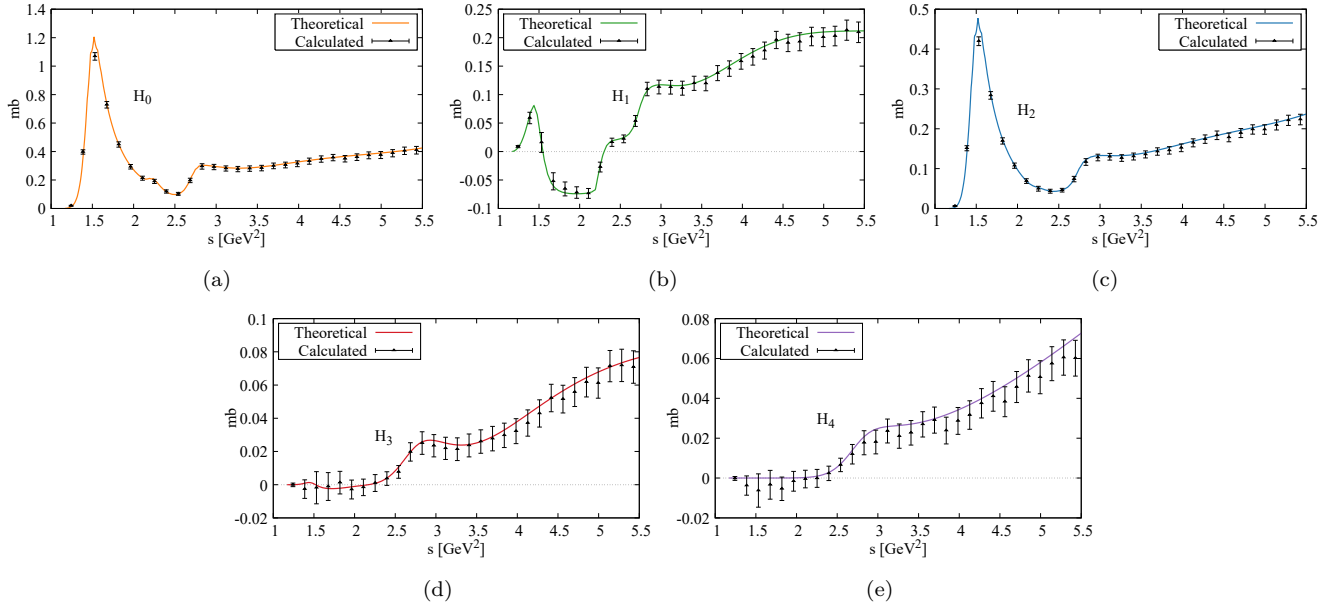


FIG. 1: Moments calculated from the histograms in z and s from the data, for $N_{\text{tot}} = 2 \cdot 10^5$ and $n_s = n_z = 30$, compared with the theoretical values calculated from Eqs. (9) with the partial waves of the model. The error bars are given by \sqrt{N} , where N is the number of events per energy bin, multiplied by the corresponding normalization constant.

higher-order moments, such as $H_3(s)$ and $H_4(s)$, are almost identically zero up to approximately $s \sim 2.5 \text{ GeV}^2$. Therefore, it would seem that up to this energy, we have an effective $\ell_{\text{max}} = 1$ in our model. We will discuss this further later.

B. Barrelet Zeros

At this point, we know all the non-zero moments, and we could simply solve the system of Eqs. (9) and find $a_0(s)$, $a_1(s)$ and $a_2(s)$. This procedure needs to be independently evaluated for each value of energy. If we observe closely, we have only five equations, so we will not be able to unambiguously determine the real and imaginary parts of all the partial waves. We have to solve this by imposing a global phase for the three waves, which can be the one that suits us best. In fact, since the differential cross-section depends on the square of the modulus of the amplitude, we cannot know the partial waves beyond a common phase. In our case, we will set the global phase such that the S -wave is real and positive. That leaves us with five unknowns and five equations to solve them. While possible, this is a poor approach, as solving this system can become excessively complicated for larger ℓ_{max} . A more suitable approach would be precisely the one mentioned in the introduction of this work, which originates from the article [1].

According to Eq. (2), the amplitude $A(s, z)$ is a polynomial of order ℓ_{max} in z , and thus, with ℓ_{max} complex

roots. For $\ell_{\text{max}} = 2$:

$$\begin{aligned} A(s, z) &= a_0(s) + 3a_1(s)z + \frac{5}{2}a_2(3z^2 - 1) \\ &= \mathcal{N}_0(z - z_1)(z - z_2). \end{aligned} \quad (14)$$

Matching the coefficients we obtain the relation between the roots (also called *Barrelet Zeros*) and the partial waves:

$$a_2(s) = \mathcal{N}_0 \left(\frac{2}{15} \right), \quad (15a)$$

$$a_1(s) = -\mathcal{N}_0 \left(\frac{z_1 + z_2}{3} \right), \quad (15b)$$

$$a_0(s) = \mathcal{N}_0 \left(z_1 z_2 + \frac{1}{3} \right). \quad (15c)$$

This is, if we can extract the roots z_i , we obtain the partial waves. Note that the roots are in general complex. To determine the ℓ_{max} roots and the constant \mathcal{N}_0 experimentally, we know the differential cross-section, but it is a real polynomial of order $2\ell_{\text{max}}$, so the roots will come in pairs (z_i, z_i^*) :

$$\frac{d\sigma}{d\Omega}(s, z) = \frac{\mathcal{N}_0^2}{16\pi^2 s} \prod_{i=0}^{\ell_{\text{max}}} (z - z_i)(z - z_i^*). \quad (16)$$

This will lead to the appearance of ambiguities, as we have to choose one root from each pair (z_i, z_i^*) . These sum up to $2^{\ell_{\text{max}}}$ possible combinations, each of which would yield the same differential cross-section but different partial waves. From these initial ambiguities, we

can discount the trivial ones, originated from calculating the modulus $|A(s, z)|$ in Eq. (1). That is, we will not count as different combinations those that lead us to $a_\ell(s)$ or $a_\ell^*(s)$. This reduces the number of ambiguities by half. For a general ℓ_{\max} , we will encounter $2^{\ell_{\max}-1}$ insurmountable ambiguities. In our case ($\ell_{\max} = 2$) we will have to deal with two of them. In more advanced practical cases, additional boundary conditions could be imposed, regarding the continuity and differentiability of the waves, to select the solution with the most physical sense. For this simple case, we will suffice by validating that one of the two obtained options coincides with the theoretical model, for each energy bin.

In practice, it might not be possible to analytically factorize the differential cross-section, so the roots are generally obtained numerically. In our case, we developed a code that evaluates a given real polynomial and minimizes it based on predefined parameters to return the complex roots, using the Minuit (Function Minimization and Error Analysis) program, version 94.1 [8].

The determination of the errors associated with the partial waves can be carried out based on the errors of the moments $\delta H_L(s)$. By deriving Eqs. (9), we arrive to linear dependences between $\delta H_L(s)$ and the uncertainties of the partial waves, which will have real and imaginary parts $\delta a_l^{r,i}(s)$ (except for $\delta a_0(s)$, which is real according to our chosen global phase):

$$(16\pi^2 s)\delta H_0 = 2a_0\delta a_0 + 6[a_1^r\delta a_1^r + a_1^i\delta a_1^i] + 10[a_2^r\delta a_2^r + a_2^i\delta a_2^i], \quad (17a)$$

$$(16\pi^2 s)\delta H_1 = 2a_0\delta a_1^r + 2a_1^r\delta a_0 + 4[a_1^r\delta a_2^r + a_2^r\delta a_1^r + a_1^i\delta a_2^i + a_2^i\delta a_1^i], \quad (17b)$$

$$(16\pi^2 s)\delta H_2 = 2a_2^r\delta a_0 + 2a_0\delta a_2^r + \frac{12}{5}[a_1^r\delta a_1^r + a_1^i\delta a_1^i] + \frac{20}{7}[a_2^r\delta a_2^r + a_2^i\delta a_2^i], \quad (17c)$$

$$(16\pi^2 s)\delta H_3 = \frac{18}{7}[a_1^r\delta a_2^r + a_2^r\delta a_1^r + a_1^i\delta a_2^i + a_2^i\delta a_1^i], \quad (17d)$$

$$(16\pi^2 s)\delta H_4 = \frac{20}{7}[a_2^r\delta a_2^r + a_2^i\delta a_2^i]. \quad (17e)$$

The previous system can be expressed in the following matrix form:

$$(16\pi^2 s) \begin{pmatrix} \delta H_0 \\ \delta H_1 \\ \delta H_2 \\ \delta H_3 \\ \delta H_4 \end{pmatrix} = X \begin{pmatrix} \delta a_0 \\ \delta a_1^r \\ \delta a_1^i \\ \delta a_2^r \\ \delta a_2^i \end{pmatrix}, \quad (18)$$

where X is the matrix:

$$\begin{pmatrix} 2a_0 & 6a_1^r & 6a_1^i & 10a_2^r & 10a_2^i \\ 2a_1^r & 2a_0 + 4a_2^r & a_2^i & a_1^r & a_1^i \\ 2a_2^r & (12/5)a_1^r & (12/5)a_1^i & 2a_0 + (20/7)a_2^r & (20/7)a_2^i \\ 0 & (18/7)a_2^r & (18/7)a_2^i & (18/7)a_1^r & (18/7)a_1^i \\ 0 & 0 & 0 & (20/7)a_2^r & (20/7)a_2^i \end{pmatrix}. \quad (19)$$

Thus, to calculate $\delta a_l^{r,i}(s)$, we simply need to find X^{-1} .

This approach requires prior knowledge of the maximum number of partial waves ℓ_{\max} present in each energy bin, which, as we have seen, does not have to be constant. Indeed, up to $s \sim 2.5 \text{ GeV}^2$, $H_3(s)$ and $H_4(s)$ are so small our model can be understood with an effective ℓ_{\max} equal to 1. The determination of ℓ_{\max} can be automated for each energy by selecting the last non-zero $H_L(s)$, then factoring the resulting differential cross-section and obtaining the *Barrelet Zeros* through the relations in Eqs. (15). In our case, however, we preferred a more practical solution by adding a small constant to the D -wave over the entire energy range, ensuring it was non-zero at any point, and subsequently subtracting it from the results. This way, we forced the effective ℓ_{\max} to be equal to 2 everywhere, and our equations remained valid. However, the moments in Fig. (1) were calculated from a data set without the added constant, in order to be more realistic and to facilitate comparison with the analytical result.

The original model from [3], used to generate the data, has a complex S -wave. To better compare our results, as it is shown at the Fig. (2), we cannot keep our S -wave as a positive real number. We will have to multiply our waves and their uncertainties by another global phase, extracted from [3] to match them. This does not change the physics we have found; as we have said, we can multiply the partial waves by any global phase that facilitates our job.

Looking at Fig. 2 we can see that, for the vast majority of energy values, at least one of the two represented points coincides with the theoretical curve. We have represented our two existing ambiguities with different colors, but we cannot ensure which color will match the curve beforehand, so this distinction should not be understood as a separation between “the good one” and “the bad one”. We also observe that, similar to what happened with the moments, as ℓ increases, the partial waves become smaller. In this case, this does not have such a clear impact on the perspective of the error bars, as these also depend on the partial waves magnitude.

As we expected from having an effective $\ell_{\max} = 1$, the higher-order ones are mostly zero up to approximately $s \sim 2.5 \text{ GeV}^2$, after subtracting the previously mentioned constant.

IV. CONCLUSIONS

We have conducted a thorough analysis of a simulated hadron scattering experiment, starting from the data generation and subsequently extracting the same partial waves used to generate it. All procedures to achieve the obtained results have been discussed, and the identified ambiguities have been properly introduced and justified. In this regard, since at least one of the obtained points for each energy bin coincides with the theoretical curve, considering the calculated errors, it can be established that the results are valid and the method works properly.

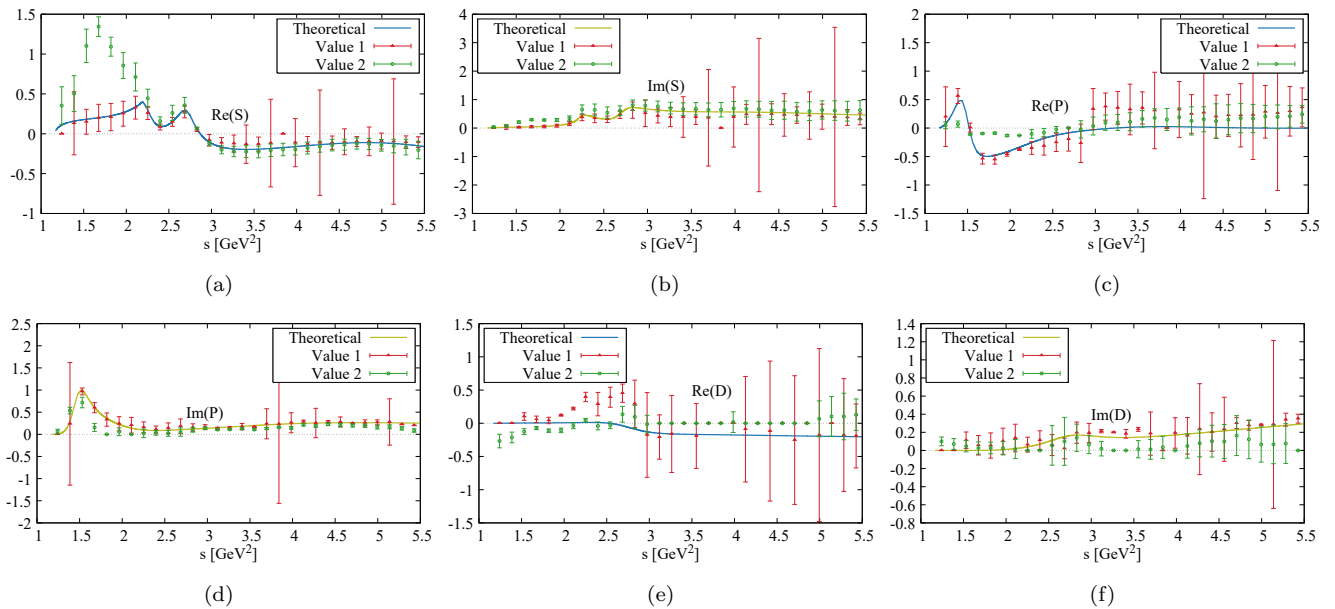


FIG. 2: Real and imaginary parts of the partial waves of the model, compared to the theoretical ones. There have been represented, in different colors, the two existing ambiguities for each energy bin and their respective uncertainties. All the partial waves are dimensionless.

It should be noted that, in a experimental situation in a laboratory, there would be other practical aspects that have not been taken into account in the development of this work, such as the acceptance of the detector recording the particles.

Also, it should be mentioned that, while the total number of events, N_{tot} , and the chosen energy bins, n_s , should not significantly affect the obtained results, they would affect the size of the errors and their accuracy. In principle, we would expect that for a higher N_{tot} , the errors would decrease, and with a higher n_s , as events are distributed more across the energy range, they should increase. In general, the choice of these parameters will depend on the required precision and the resources available to each individual.

We also wanted to mention additional objectives that, with more time, we could have studied, such as the possibility of having repeated our analysis, directly fitting the partial waves to the expression of the differential cross-section using one of the statistical techniques al-

ready mentioned, like the Maximum Likelihood Estimation. This might be a more professional and realistic approach when dealing with this type of data. In addition, seeking further realism, we could have considered the possibility of conducting a similar study with polarized particles with spin, and even adding interactions with more than two particles.

With this article, we hope to have presented a basic yet comprehensive guide on how to prepare and analyze data in hadron spectroscopy.

Acknowledgments

First, I would like to thank my tutor, Vincent, who has always been open to helping me with all the problems that have arisen during the preparation of this work. I would also like to thank my friends and partner, who have supported and aided me whenever possible.

-
- [1] E. Barrelet, *Nuovo Cim. A* **8** (1972), 331-371 doi:10.1007/BF02732655
 - [2] G. Hohler, F. Kaiser, R. Koch and E. Pietarinen, *Phys. Daten* **12N1** (1979), 1
 - [3] R. L. Workman, M. W. Paris, W. J. Briscoe and I. I. Strakovsky, *Phys. Rev. C* **86** (2012), 015202 doi:10.1103/PhysRevC.86.015202 [arXiv:1202.0845 [hep-ph]].
 - [4] A. D. Martin and T. D. Spearman, North-Holland Publishing Co., 1970, ISBN 978-0-7204-0157-8
 - [5] R. L. Workman *et al.* [Particle Data Group], *PTEP* **2022** (2022), 083C01 doi:10.1093/ptep/ptac097
 - [6] R. J. Barlow, *CERN Yellow Rep. School Proc.* **5** (2020), 149-197 doi:10.23730/CYRSP-2021-005.197 [arXiv:1905.12362 [physics.data-an]].
 - [7] G. Bohm and G. Zech, doi:10.3204/PUBDB-2017-08987
 - [8] F. James and M. Roos, *Comput. Phys. Commun.* **10** (1975), 343-367 doi:10.1016/0010-4655(75)90039-9